Multi-Instrument Observation of the 2021 May 7 Solar Eruption

A. F. Battaglia[1,2], S. Krucker[1,3], A. Warmuth[4], P. Massa[5], E. Perracchione[5], M. Piana[5], A. M. Massone[5], W. Wang[1,6], J. Saqri[7], E. C. M. Dickson[7], H. Xiao[1], A. M. Veronig[7], M. Battaglia[1], E. Podladchikova[8], L. Harra[8], and the STIX Team

[1]FHNW, Windisch, Switzerland [2]ETHZ, Zurich, Switzerland [3]UCa, Berkeley, USA [4]AIP, Potsdam, Germany [5]UniGe, Genova, Italy [6]SESS, Beijing, China [7]UniGraz, Graz, Austria [8]PMOD/WRC, Davos, Switzerland

Introduction

We report on the solar eruption on 2021 May 7 (SOL2012-05-07T18) that has been observed from Earth and also by STIX (Spectrometer/telescope for Imaging X-rays; Krucker et al., 2020), the hard X-ray telescope onboard Solar Orbiter. With the STIX instrument, the study focuses on the solar flare, since STIX allows to perform imaging spectroscopy of hard X-ray photons between 4 to 150 keV. In this energy range, it is possible to diagnose the hottest plasma in the solar corona (8 MK and above; Battaglia et al., 2021) and also estimate the energy of the electrons that are accelerated during solar flares. The first reconstructed STIX images are presented and with hard X-ray spectroscopy we discuss the different energies governing the flaring event.

The effects of the violent processes dominating the eruption generated a spectacular large scale coronal wave that is clearly observable in EUV. Here we take a first look to it and estimate its propagation speed.

Multi-wavelength time evolution

An overview of the multi-wavelength time evolution of the solar flare is given in Fig. 1.

The GOES soft X-ray lightcurves on the topmost panel show thermal emission that is the gradual behavior caused by heated plasma filling coronal loops. The derivative of the GOES 1-8 Å, the black dotted line, describes the heating rate involved in the early stages of the flare process. Likewise, the middle panel also shows thermal emission, but this time with two different instruments: STIX and Hinode/XRT. The peak times of the various thermal lightcurves are clearly different: this is intrinsically related to the multi-thermal nature of solar flares and the temperature responses of the different instruments.

Emission mostly coming from the nonthermal bremsstrahlung is illustrated in the bottom panel of Fig. 1. The STIX 18-22 keV lightcurve shows a typical long lasting profile, of about 20 minutes, which nicely agrees with both the AIA 1600 Å and the derivative of the GOES 1-8 Å time profiles. Indeed, the emission detected by the 1600 Å passband mostly comes from the chromospheric heights, which is consistent with the scenario of the downward flare-accelerated electrons interacting with the more dense chromosphere. Moreover, the agreement with the derivative of the GOES 1-8 Å lightcurve is consistent with the idea that the heating rate of the flare loops is caused by the energy deposited from these downward flare-accelerated electrons interacting with the chromosphere. Emission up to 50 keV is observed in the main nonthermal peak and also, less intensively, in the last one, as shown by the STIX 36-50 keV lightcurve.

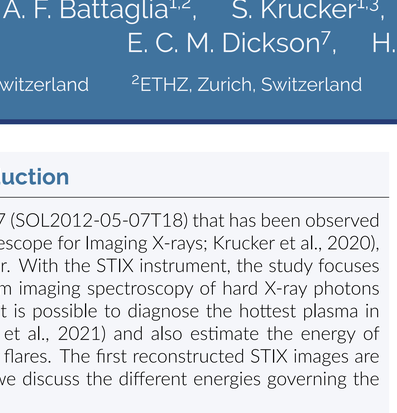

Figure 1: The GOES soft X-ray profiles (*top*) together with the STIX 6-7 keV, XRT Al thick and XRT Be thick lightcurves (*middle*) show the thermal emission of the solar flare, while STIX 18-22 keV, STIX 36-50 keV and the AIA 1600 Å (*bottom*) outline the impulsivity of the event, indicative of nonthermal brehmsstrahlung emission. STIX times are adjusted to the light travel time to Earth.

Preliminary STIX hard X-ray imaging

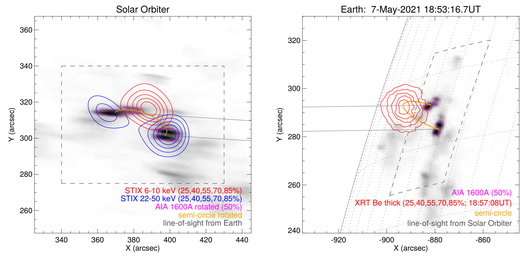

Figure 2: Imaging of the flare event seen from different look directions: Solar Orbiter (*left*) and Earth (*right*). The STIX nonthermal (blue) and thermal (red) sources are overlayed on the rotated AIA 1600 Å map as it would be seen from Solar Orbiter. In order to guide the eye, in orange, the same semi-circle connecting the flare ribbons is drawn as a proxy of the flare loops.

Despite the calibration of the STIX imaging system is still ongoing, in Fig. 2 we report the first reconstructed images of the instrument. The left panel shows the AIA 1600 Å as it would be seen from the Solar Orbiter vantage point, over which we plotted the nonthermal (blue) and thermal (red) reconstructed sources, using the new Maximum Entropy Method algorithm based on visibilities (Massa et al., 2020). Despite the absolute location of the source has still an uncertainty of up to $\sim$ 30 arcsec (the current reconstructed image has been manually shifted), with the reconstructed image that we obtain at the current stage of the calibration, it is possible to get information on the source shape, size and orientation, and the relative separation between thermal and nonthermal emission, which in the case of Fig. 2 are consistent with the flare ribbons seen in the AIA 1600 Å map.

Large scale coronal wave

A large scale coronal wave is associated with the solar eruption, as depicted in Fig. 3. The propagation speed has been computed along two different directions: `dir1` (red arrow) and `dir2` (blue arrow). By taking into account projection effects and assuming surface propagation, we found consistent values for the speed along `dir1` from both EUVI and AIA maps. Contrarily, the speed along `dir2` is smaller compared to the previous one, which may indicate that the emission comes also from the corona, as it can be seen from the AIA image. This suggests that the propagation vector can have a component also in the radial direction.

The linear fits of the `dir1` in the distance-time plot confirm that the launch of the wave is close to the impulsive STIX nonthermal peak time, which is related to the energy input by nonthermal electrons. This temporal association is in agreement with the result of Warmuth (2010), in which the launch of 24 out of 27 waves happened within $\pm$4 minute interval around the hard X-ray peak. Despite the good time correlation, we note that the wave is not launched by the flare, but by the associated CME.

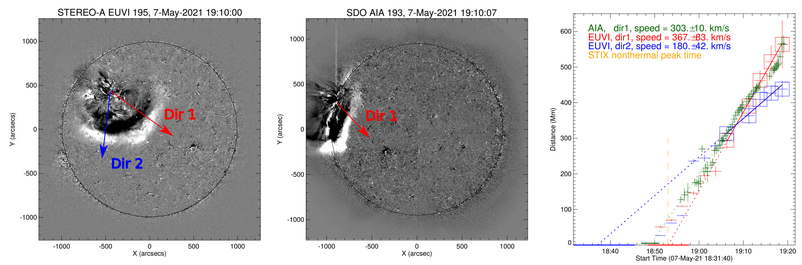

Figure 3: The running difference maps of the STEREO-A/EUVI 195 Å (*left*) and SDO/AIA 193 Å (*middle*) passbands show a time instant of the propagating large scale coronal wave. The propagation speed (*right*) has been deduced along two different directions.

Energetic considerations of the flare

The hard X-ray spectroscopic analysis that is shown in Fig. 4 is done with the forward fitting software OSPEX of the SSWIDL package, which is still in the process of being adapted for usage with the STIX data. The leftmost panel depicts two forward fitted spectra at different times: the first time is fitted with the single thermal `'vth'` and thick target model `'thick2'` at higher energies, while the second time with two single thermal fits and a thick target model.

The panel in the middle shows the time evolution of the temperature, emission measure and, at the time instants where a thick target model can be fitted, the electron flux. In the temperature and emission measure plots, the orange curves represent the parameters deduced from GOES, while black and red correspond to the two single thermal components, hot and super-hot, respectively, deduced by STIX.

By combining spectroscopy and imaging, it is possible to estimate the various forms of energies involved in the flare process. The rightmost panel of Fig. 4 shows that the injected nonthermal energy is larger than the peak thermal energy. This is consistent with the scenario of beam-driven evaporation, where the kinetic energy of nonthermal electrons is converted into thermal energy of plasma that is then expanding from the chromosphere into the corona.

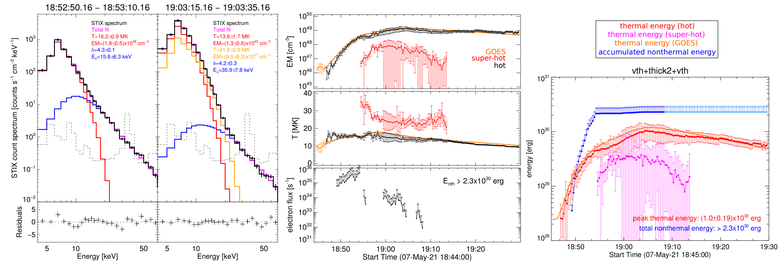

Figure 4: Time evolution analysis of the spectroscopic models and energies involved in the flare process. The left panel depicts two spectra at different times as examples of STIX spectroscopic fits. In the central panel, the time evolution of these spectroscopic fits is shown. Finally, the rightmost panel compares the derived nonthermal energy input by flare-accelerated electrons with the thermal energy content in flare loops. We note that for the spectroscopic fitting, no albedo correction has been taken into account yet.

Conclusions

The STIX team has been using SOL2021-05-07T18 to test the STIX instrument performance and to verify the current state of instrument calibration. While the calibration efforts are still ongoing, initial results show that the instrument has all functionalities as designed.

The presented results are in agreement with previous studies, but offer for the first time X-ray flare observations from a different vantage point allowing us to reconstruct the flare geometry in 3D.

References

Battaglia, A. F., Saqri, J., Massa, P., et al. 2021, accepted (A&A)
Krucker, S., Hurford, G. J., Grimm, O., et al. 2020, A&A, 642, A15
Massa, P., Schwartz, R., Tolbert, A. K., et al. 2020, A&A, 894, 46
Warmuth, A. 2010, Advances in Space Research, 45, 527